Published in final edited form as:

J Neuroimmune Pharmacol. 2016 June ; 11(2): 316–331. doi:10.1007/s11481-016-9664-y.

Cannabinoids occlude the HIV-1 Tat-induced decrease in GABAergic neurotransmission in prefrontal cortex slices

Changqing Xu[1], **Douglas J Hermes**[1], **Ken Mackie**[2], **Aron H Lichtman**[3], **Bogna M Ignatowska-Jankowska**[4], and **Sylvia Fitting**[1,*]

[1]Department of Psychology & Neuroscience, University of North Carolina Chapel Hill, Chapel Hill, NC 27599

[2]Department of Psychological & Brain Sciences, Indiana University, Bloomington, IN 47405

[3]Department of Pharmacology & Toxicology, Virginia Commonwealth University, Richmond, VA 23298

[4]Edmond and Liliy Safra Center for Brain Sciences, Hebrew University of Jerusalem, Jerusalem, Israel

Abstract

In the era of combined antiretroviral therapy (cART), human immunodeficiency virus type 1 (HIV-1) is now considered a chronic disease that specifically targets the brain and causes HIV-1-associated neurocognitive disorders (HAND). Endocannabinoids exhibit neuroprotective and anti-inflammatory properties in several central nervous system (CNS) disease models, but their effects in HAND are poorly understood. To address this issue, whole-cell recordings were performed on young (14 – 21 day old) C57BL/6J mice. We investigated the actions of the synthetic cannabinoid WIN55,212-2 (1 μM) and the endocannabinoid N-arachidonoyl ethanolamine (anandamide; AEA, 1 μM) in the presence of HIV-1 Tat on GABAergic neurotransmission in mouse prefrontal cortex (PFC) slices. We found a Tat concentration dependent (5 – 50 nM) decrease in the frequency and amplitude of miniature inhibitory postsynaptic currents (mIPSCs). The cannabinoid 1 receptor (CB_1R) antagonist rimonabant (1 μM) and zero extracellular calcium prevented the significant Tat-induced decrease in mIPSCs. Further, bath-applied WIN55,212-2 or AEA by itself, significantly decreased the frequency, but not amplitude of mIPSCs and/or spontaneous IPSCs (sIPSCs), and

Corresponding Author: Sylvia Fitting, Ph.D., Dept. Psychology and Neuroscience, University of North Carolina, Chapel Hill, Chapel Hill, NC 27599, Phone: 919-962-6595, Fax: 919-962-2537, sfitting@email.unc.edu.

Author contributions: CX, SF, BMIJ designed the research; CX performed the electrophysiology experiments; DJH performed the immunohistochemistry experiments, CX, DJH analyzed the data; CX, DJH, KM, AHL, BMIJ, SF interpreted the data; SF wrote the paper; CX, KM, AHL, BMIJ, SF discussed and edited the paper.

The authors declare no competing financial interests.

Conflict of Interest

Changqing Xu declares that he has no conflict of interest.
Douglas J Hermes declares that he has no conflict of interest.
Ken Mackie declares that he has no conflict of interest.
Aron H Lichtman declares that he has no conflict of interest.
Bogna M Ignatowska-Jankowska declares that she has no conflict of interest.
Sylvia Fitting declares that she has no conflict of interest.

Ethical approval

All applicable international, national, and/or institutional guidelines for the care and use of animals were followed.

occluded a further down-regulation of IPSCs by Tat. Pretreatment with rimonabant but not the CB_2R antagonist AM630 (1 μM) prevented the WIN55,212-2- and AEA-induced decrease in IPSCs frequency without any further Tat effect. Results indicated a Tat-induced decrease in GABAergic neurotransmission, which was occluded by cannabinoids via a CB_1R-related mechanism. Understanding the relationship between Tat toxicity and endocannabinoid signaling has the potential to identify novel therapeutic interventions to benefit individuals suffering from HAND and other cognitive impairments.

Keywords

HIV-1 Tat; cannabinoid; GABA neurotransmission; prefrontal cortex; calcium; cannabinoid 1 receptor

Introduction

Human immunodeficiency virus type 1 (HIV-1) infects the brain and, despite combined antiretroviral therapy (cART), 30–50% infected individuals suffer from HIV-1-associated neurocognitive disorders (HAND) (Ellis et al., 2007; Heaton et al., 2011). Specifically in the post-cART era, cortical deficiencies have been observed in addition to subcortical deficits with HIV-1 patients displaying marked decreases in executive function, memory consolidation, and attention, all of which are associated with the prefrontal cortex (PFC) (Heaton et al., 2011). Synaptodendritic damage with markers of neuronal injury, such as injury to synapses and dendrites, underlie the neurocognitive impairments seen in HIV-1-infected individuals and are strongly associated with HAND (Masliah et al., 1997; Ellis et al., 2007). Disturbance of neurotransmitter systems and circuits play an important role in synaptodendritic damage and neuro-acquired immune deficiency syndrome (neuroAIDS). Alterations have been reported in glutamatergic neurotransmission (Ferrarese et al., 2001; Ernst et al., 2010), as well as in serotonergic systems (Murray, 2003; Schroecksnadel et al., 2007) and in dopaminergic circuits (Berger and Arendt, 2000; Nath et al., 2000; Wang et al., 2004; Gelman et al., 2006). The GABAergic inhibitory system in neuroAIDS has recently been implicated with dysregulated GABAergic neurotransmission in HIV-1 positive individuals, specifically in the neocortex (Gelman et al., 2012). A significant downregulation of pre- and post-synaptic GABAergic inhibitory systems was reported selectively in the frontal neocortex of HIV-1 positive patients with neurocognitive impairments (Gelman et al., 2012). The observation that both presynaptic and postsynaptic GABA markers were regulated (Gelman et al., 2012) implies coordinated changes in synaptic tone (plasticity) of inhibitory neocortical circuits.

Preclinical animal studies have demonstrated that the expression of the HIV-1 transactivator of transcription (Tat) in transgenic rodent models induced sub-lethal neuronal injury and reduced synaptic connectivity (Fitting et al., 2010; Fitting et al., 2013; Roscoe et al., 2014), resulting in cognitive and behavioral deficits (Carey et al., 2012; Fitting et al., 2013; Hahn et al., 2013; Moran et al., 2013; Paris et al., 2015). *In vitro*, Tat produces excitotoxicity through diverse mechanisms, including binding to the low-density lipoprotein receptor-related protein (LRP) (Kim et al., 2008), the activation of N-methyl-D-aspartate (NMDA) receptors

(Magnuson et al., 1995; Haughey et al., 2001; Perez et al., 2001; Li et al., 2008; Aksenov et al., 2012) and α-amino-3-hydroxy-5-methyl-4-isoxazolepropionic acid (AMPA) receptors (Longordo et al., 2006; Fitting et al., 2014), leading to increases in $[Na^+]_i$, mitochondrial instability, and excessive Ca^{2+} influx (Perez et al., 2001; Haughey and Mattson, 2002; Fitting et al., 2014), subsequent dendritic damage (Kruman et al., 1998; Haughey et al., 2001; Bertrand et al., 2014; Fitting et al., 2014) and synapse loss (Kim et al., 2008). However, the effects of Tat on GABAergic neurotransmission are not well known.

The persistence of HAND in the era of cART raises questions about the causes and treatment of HIV-1-related brain disorders and the extent to which neuronal dysfunction and injury are reversible (Ellis et al., 2007). Upregulation of the endogenous cannabinoids N-arachidonoyl ethanolamine (anandamide; AEA) and 2-arachidonoyl glycerol (2-AG) have protective properties in neurodegenerative disorders, including multiple sclerosis, Parkinson, and Alzheimer disease models (Grant and Cahn, 2005; Scotter et al., 2010; Maroof et al., 2013; Pertwee, 2014; Xu and Chen, 2015). Endocannabinoids act predominantly via cannabinoid 1 (CB_1) and/or cannabinoid 2 (CB_2) receptors, although involvement of transient receptor potential (TRP) channels (Higgins et al., 2013; Yuan and Burrell, 2013; Kano, 2014) and/or other G-protein-coupled receptors (GPCRs) (Chevaleyre et al., 2006; Harkany et al., 2008; Ross et al., 2012) have been reported. CB_1 receptors (CB_1Rs) are the most abundant G-coupled receptors in the brain, with the highest concentration in regions such as the cortex, hippocampus, and basal ganglia (Matsuda et al., 1990). CB_1R are expressed in both excitatory (glutamatergic) and inhibitory (GABAergic) cells (Kano et al., 2009) predominantly at presynaptic terminals (Di Marzo et al., 2015). The neuroprotective properties of cannabinoids in the presence of the HIV-1 envelope glycoprotein gp120 has been studied in several cellular and animal models (Kim et al., 2011; Hu et al., 2013; Avraham et al., 2014). There is support for existing signaling pathways from CB_1R activation to inhibition of NMDA calcium influx (Liu et al., 2009), thus decreasing neuronal injury. Further, inhibition of glutamatergic and GABAergic neurotransmission by cannabinoid agonists has been documented in the PFC (Auclair et al., 2000; Kano et al., 2009; Kovacs et al., 2012; Lee et al., 2015). In the present study we examined the effects of the synthetic cannabinoid WIN55,212-2 (1 μM) and the endocannabinoid AEA (1 μM) on GABAergic neurotransmission in a model of neuroAIDS. Not much is known about how Tat interacts with cannabinoids and whether the potential protective effects of cannabinoids in the presence of Tat can be attributed to the effects on the GABAergic system. Results indicated a Tat-induced decrease in GABAergic neurotransmission, which was occluded by cannabinoids via a CB_1R-related mechanism.

Materials and Methods

Experiments were conducted in accordance with the NIH Guide for the Care and Use of Laboratory Animals (National Research Council, 2011). All procedures were approved by the University of North Carolina at Chapel Hill.

Immunohistochemical staining of cannabinoid 1 receptor (CB_1R)

C57BL/6J mice were anesthetized with isofluorane and perfused with 4% paraformaldehyde. Brains were removed and post-fixed in 4% paraformaldehyde (for 2 h at 4 °C), then washed in 1x PBS several times and incubated for at least 32 h in 20% sucrose in PBS. Brains were embedded in Tissue-Tek O.C.T. compound, frozen, and stored at −80°C until cut. Coronal brain sections (30 μm) containing PFC were cut on a Leica CM3050S cryostat (Leica, Deerfield, IL). Sections were exposed to blocking buffer (1% normal goat serum, 4% bovine serum albumin, 0.4% Triton X-100 in PBS) for 1.5 h. Sections were incubated with primary antibodies against MAP2 (mouse, Millipore, MAB378; 1:200) and the rat CB_1R-NH (raised to amino acids 1-77 of the N-terminus; rabbit, 1:500; Tsou et al., 1998), diluted in blocking buffer, overnight at 4 °C. Primary antibodies were detected using appropriate secondary antibodies conjugated to either goat-anti-mouse Alexa 488 (Molecular Probes, O-6380, 1:1000) or goat-anti-rabbit Alexa 594 (Molecular Probes, A11012; 1:1000), respectively. Secondary antibodies were diluted in blocking buffer and applied to the sections for 1 h at room temperature. Cell nuclei were visualized with Hoechst 33342 (Molecular Probes, H3570, exposed for 3 min). Tissue sections were washed thoroughly with PBS and coverslipped with ProLong Gold (Molecular Probes, P36930). Confocal immunofluorescent images were acquired using a Zeiss LSM T-PMT laser scanning confocal microscope equipped with a 63x oil immersion objective and configured to an Axio Observer Z.1 microscope (Zeiss, Thornwood, NY). Images were collected using ZEN 2010 blue Edition software (Carl Zeiss, Inc., Thornwood, NY) and created from multiple z-stacks taken through the thickness of the section, then converted into orthogonal projection images compressed into single projected images to better show the cells in their entirety. Adobe Photoshop CS6 Extended 13.0 software (Adobe Systems, Inc.; San Jose, CA) was used to edit the images.

Slice Electrophysiology

Prefrontal cortex (PFC) slices—Brain PFC slices were prepared from male and female postnatal day P14 – 24 C57BL/6J mice (The Jackson Laboratory, Bar Harbor, ME). The brain was removed after decapitation and placed into ice-cold sucrose buffer containing (in mM): 254 sucrose,10 D-glucose, 26 $NaHCO_3$, 2 $CaCl_2$, 2 $MgSO_4$, 3 KCl, and 1.25 NaH_2PO_4, saturated with 95% O_2/5% CO_2, at pH 7.4, 300 mOsm. Coronal PFC slices (300 μm thick, Figure 1a) were cut with a VT 1000S microtome (Leica, Deerfield, IL). Slices were transferred immediately into a holding chamber and were incubated at 32 to 33 C for a 30-min recovery period in a mixture of 50% sucrose saline and 50% artificial cerebrospinal fluid (aCSF) containing (in mM): 128 NaCl, 10 D-glucose, 26 $NaHCO_3$, 2 $CaCl_2$, 2 $MgSO_4$, 3 KCl, and 1.25 NaH_2PO_4. Slices were then placed on a nylon mesh, submerged in normal aCSF bubbled continuously with 95% O_2/5% CO_2, and maintained at room temperature (~21–24°C) until whole-cell patch-clamp recording (30 min to 5 h).

Electrophysiological recordings—Slices were transferred to a submersion-type recording chamber (Warner Instruments, Hamden, CT) on a Siskiyou 4080P fixed-stage system (Grants Pass, OR), secured beneath a nylon harp, and perfused with aCSF heated to 30 to 33°C with an inline heater (Warner SC-20, Hamden, CT) at a rate of 2 to 3 mL per min. As depicted in Figure 1, recordings were taken from the medial (m)PFC of layer 2/3

(Figure 1b). Layer 2/3 pyramidal neurons are known to receive dense inhibitory synaptic input from a rich variety of interneurons to provide tight control of neuronal excitability (Olah et al., 2009; Petersen and Crochet, 2013). PFC pyramidal neurons were identified visually by using an Axio Examiner A1 microscope (Zeiss, Thornwood, NY) equipped with a 40x water-immersion objective coupled with an infrared differential interference contrast and an integrated Dodt gradient camera system (Figure 1c). Whole-cell patch-clamp recordings from PFC neurons were established using a MultiClamp 700B amplifier (Axon Instruments, Union City, CA). Membrane current and potential signals were digitized and analyzed with Digidata 1550A and pClamp 10.0 systems (Molecular Devices, Sunnyvale, CA). Patch pipettes of ~5 MΩ were pulled with a PC-10 puller (Narishige, Greencale, NY). The pipette solution had the following composition (in mM) unless otherwise stated: 140 KCl, 0.1 $CaCl_2$, 5 EGTA, 10 HEPES, 4 ATP-Mg^{2+}, 0.4 GTP-2Na^+, 1 QX314 (Lidocaine N-ethyl bromide), pH 7.2, 290 mOsm. QX314 was added to the pipette solution to block the $GABA_B$R-mediated currents and to prevent the generation of Na^+-dependent action potentials. Under these conditions, miniature postsynaptic currents (mPSCs) were acquired in aCSF containing tetrodotoxin (TTX, 1 μM) at a holding potential of −70 mV. To record spontaneous inhibitory postsynaptic currents (sIPSCs) and mIPSCs, glutamate receptor antagonists DNQX (20 μM) and AP-5 (20 μM) were added to aCSF. Drugs were administered by bath application. Synaptic currents were collected for 5 min for each experimental condition. Access resistance (<25 MΩ) was regularly monitored during recordings, and cells were rejected if resistance changed >15% during the experiment. If the access resistance increased during the course of the experiment and caused significant reductions in the synaptic current amplitudes, efforts were made to improve access (such as applying additional suction or slight positive pressure); if this failed, the experiment was discontinued.

Acquisition and analysis of synaptic currents—Spontaneously occurring synaptic currents were filtered at 2 kHz, and digitized at 10 kHz using Digidata 1550A. Off-line analysis of synaptic currents was performed using the Minianalysis software (Version 6.0.8; Synaptosoft, Decatur, GA). Synaptic currents were screened automatically using an amplitude threshold of 3 pA. Events were then visually screened to ensure that the analysis was not distorted by changes in noise level or by membrane fluctuations. If the background noise increased during the recording, the data from that cell were discarded. The data generated from these measurements were used to plot cumulative probability amplitude and inter-event interval graphs, with each distribution normalized to a maximal value of 1. Cumulative probability plots obtained under different experimental conditions were compared using the nonparametric Kolmogorov –Smirnov test (KS-T), which estimates the probability that two cumulative distributions differ from each other by chance alone (Xu et al., 2009). All numerical values are expressed as mean ± standard error of the mean (SEM) and statistical analyses were performed by using a paired Student's *t*-tests as needed. An alpha level of $p < 0.05$ was considered significant for all statistical tests used.

Drugs

Treatments included HIV-1 Tat_{1-86} (1–50 nM, rtat HIV-1 IIIB, ImmunoDX, Woburn, MA), the synthetic cannabinoid WIN55,212-2 (1 μM, Tocris, Ellisville, MO), the endocannabinoid

anandamide (AEA, 1 μM, Tocris, Ellisville, MO), the CB_1R antagonist rimonabant (1 μM, Tocris, Ellisville, MO), and the CB_2R antagonist AM630 (1 μM, Tocris, Ellisville, MO). Cannabinoid concentrations were chosen based on preliminary experiments (data not shown) and previous studies that assessed the protective effects of cannabinoids in different disease models, including NMDA-induced increases in $[Ca^{2+}]_i$ (Zhuang et al., 2005; Liu et al., 2009), AMPA-induced excitotoxicity (Kokona and Thermos, 2015), gp120-induced synaptic loss (Kim et al., 2011), and gp120-induced dopaminergic neuronal damage (Hu et al., 2013). Tat concentrations were chosen from the range that elicited functional deficits in neurons similar to those occurring in HIV-1, and that are considered to reflect levels seen under pathological conditions (Singh et al., 2004; Fitting et al., 2014). AP-5 (DL-2-amino-5-phosphonovaleric acid, NMDA receptor antagonist, 20 μM), DNQX (6,7-dinitroquinoxaline-2,3-dione, AMPA and kainate receptor antagonists, 20 μM), and TTX (tetrodotoxin, 1 μM) were purchased from Tocris (Ellisville, MO). All drugs were dissolved in dimethyl sulfoxide (DMSO), except for HIV-1 Tat, TTX, and AP-5, which were dissolved in distilled water. All stock solutions were stored at −80 °C as frozen aliquots for less than one month. Drugs were administered by bath application. AP-5, DNQX and TTX were bath applied 20 min prior to, and for the duration of the experiment. For the experimental manipulation of extracellular calcium we used aCSF without calcium or aCSF with cadmium chloride, which blocks high and low threshold voltage-dependent calcium channels ($CdCl_2$, 200 μM, Sigma, St. Louis, MO).

Results

Immunohistochemical analysis of the distribution of CB_1R in the mouse PFC

To identify regional and cellular distribution of CB_1Rs in layer 2/3 of the mPFC, immunohistochemical stainings were conducted on PFC tissue sections. In the current study, we used a well characterized CB_1R-NH antibody (Tsou et al., 1998) to locate CB_1Rs in the mouse mPFC. The CB_1R is a G protein-coupled cannabinoid receptor highly expressed in the central nervous system (CNS) and peripheral tissues. It is particularly enriched on presynaptic terminals and decreases neurotransmitter release primarily through activation of inhibitory G proteins (thus being coupled through $G_{i/o}$ proteins; Howlett et al., 2010). The CB_1R is most abundant in the cortex, striatum, hippocampus (Matsuda et al., 1990) and has been shown to play an important role in decreasing GABAerigic neurotransmitter release in these regions (Kovacs et al., 2012; Lee et al., 2015). Cells were stained for endogenous CB_1R (red), MAP2 (green) and counterstained with Hoechst 33342 (blue) with images being taken in the mPFC of layer 2/3 where recordings were conducted (Figure 2). CB_1R staining revealed a dense axonal meshwork with CB_1Rs being localized in axons (arrow) as well as in the soma (arrowhead). The uniform distribution of these receptors on the cytoplasm and axons indicates that abundant CB_1R are present in our mPFC mouse tissue.

Tat concentration dependent effects on mIPSCs in PFC pyramidal neurons

GABAergic neurotransmission and specific synaptic proteins associated with inhibitory synapses have been shown to be altered by Tat (Fitting et al., 2013; Hargus and Thayer, 2013). To explore the effects of Tat on spontaneous and miniature $GABA_A$ receptor-mediated inhibitory postsynaptic currents (sIPSCs and mIPSCs, respectively), we performed

patch-clamp recordings on mPFC pyramidal neurons in the presence of DNQX and AP-5 (Figure 3). sIPSCs and mIPSCs were confirmed by the application of $GABA_A$ receptor antagonist bicuculline (data not shown). Tat at any concentration (5 – 50 nM) had no significant effect on the mean frequency and amplitude of sIPSCs ($n = 6$, Figure 3a). To assess mIPSCs, TTX was added to the bath to eliminate large-amplitude, action potential-dependent IPSCs. The representative traces of mIPSCs before and after Tat application are shown in Figure 3b. A concentration dependent decrease in the frequency and amplitude of mIPSCs by Tat (5 – 50 nM) was noted in the presence of TTX (Figure 3c). Tat significantly decreased the mean frequency and amplitude of mIPSCs at Tat (10 nM) and Tat (50 nM) compared to before Tat application ($n = 11$, paired t-tests, $p < 0.05$). Thus, Tat inhibits action potential-independent release of GABA concentration-dependently via presynaptic and postsynaptic mechanisms.

Effects of Tat in combination with WIN55,212-2 on mIPSCs

To explore the effects of cannabinoids in the presence of Tat on sIPSCs and mIPSCs, we performed patch-clamp recordings on mPFC pyramidal neurons with bath application of WIN55,212-2 (1 μM) following Tat (10 nM) administration. No effects were noted for the mean frequency or amplitude of sIPSCs ($n = 7$, Figure 4a). To assess mIPSCs, TTX was added to the bath to eliminate large-amplitude, action potential-dependent IPSCs. The representative traces of mIPSCs for before and after Tat application are shown in Figure 4b. The cumulative frequency and amplitude histograms for representative cells demonstrate a significant decrease in frequency and amplitude of mIPSCs with the application of Tat (KS-T, $p < 0.05$, Figure 4c). Tat significantly decreased the mean frequency of mIPSCs (from 2.60 ± 1.05 Hz to 1.54 ± 0.59 Hz, $n = 5$, paired t-test, $p < 0.05$, Figure 4d) and mean amplitude of mIPSCs (from 27.81 ± 3.91 pA to 20.74 ± 2.90 pA, $n = 5$, paired t-test, $p < 0.05$, Figure 4d), which was not affected by bath application of WIN55,212-2 following Tat treatment ($n = 5$, Figure 4d). Thus, Tat produced a significant decrease in GABAergic neurotransmission at the level of an action potential-independent release of GABA (mIPSCs, i.e. quantal release) that was not affected by the synthetic cannabinoid WIN55,212-2.

Significant effects of WIN55,212-2 on mIPSCs in PFC pyramidal neurons

It is well known that cannabinoids, such as WIN55,212-2, decrease GABAergic neurotransmission in different brain regions (Hoffman and Lupica, 2000; Chen et al., 2010; Chiu et al., 2010), but the combined effects of WIN55,212-2 followed by Tat application on GABA release is less clear. Thus, we examined IPSCs before and after WIN55,212-2 (1 μM) treatment, which was then followed by Tat (10 nM) application (Figure 5). No significant effects were noted on the mean frequency and amplitude of sIPSCs ($n = 7$, Figure 5a). mIPSCs were assessed in the presence of TTX with the representative traces for control, WIN55,212-2, and WIN + Tat shown in Figure 4b. WIN55,212-2 significantly reduced the mean frequency of mIPSC (from 1.93 ± 0.51 Hz to 1.52 ± 0.50 Hz, $n = 7$, paired t-test, $p < 0.05$, Figure 5c), which was significantly blocked by rimonabant (1 μM, $n = 9$, Figure 5c′) but not AM630 (1 μM, $n = 8$, Figure 5c″). Interestingly, no further downregulation of GABA release was noted by Tat following WIN55,212-2 application compared to WIN55,212-2 alone ($n = 7$, Figure 5c). No WIN55,212-2 and WIN + Tat effects were noted on the mean amplitude of mIPSCs in the absence or presence of rimonabant ($n = 7$, Figure 5d and $n = 9$,

Figure 5d′, respectively), which has been reported previously (Vaughan et al., 1999; Takahashi and Linden, 2000; Trettel and Levine, 2002; Chevaleyre et al., 2007; Chiu et al., 2010). When PFC slices were pretreated with AM630 a significant downregulation of the mean amplitude of mIPSCs was noted for WIN55,212-2 and WIN + Tat compared to control ($n = 8$, paired t-tests, $p < 0.05$, Figure 5d″). Thus, WIN55,212-2 produced a significant decrease in the mean frequency of mIPSCs, which was significantly blocked by the CB_1R antagonist rimonabant but not by the CB_2R antagonist AM630. No further downregulation by Tat was noted in any condition, suggesting the decrease of GABA release by Tat was occluded by WIN55,212-2.

Significant effects of AEA on mIPSCs and sIPSCs in PFC pyramidal neurons

As WIN55,212-2 is a synthetic cannabinoid, we next investigated endocannabinoid AEA (1 μM) effects in combination with Tat (10 nM) treatment (Figure 6). The representative traces of sIPSCs for control, AEA, and AEA + Tat are shown in Figure 6a. In contrast to WIN55,212-2, AEA decreased the mean frequency of sIPSCs (from 2.18 ± 0.66 Hz to 1.88 ± 0.63 Hz, $n = 7$, paired t-test, $p < 0.05$, Figure 6b), which was significantly blocked when pretreating PFC slices with the CB_1R antagonist rimonabant (1 μM, $n = 5$, Figure 6b′) but not with the CB_2R antagonist AM630 (1 μM, $n = 10$, Figure 6b″). No effects were noted for AEA on the mean amplitude of sIPSCs ($n = 7$, Figure 6c), indicating that the AEA-induced decrease in sIPSC frequency was significantly reduced by an action potential-dependent release of GABA via a presynaptic mechanism. Further, no AEA effects were noted on the mean amplitude of sIPSCs in the presence of rimonabant ($n = 5$, Figure 6c′), or in the presence of AM630 ($n = 10$, Figure 6c″). Tat revealed no further downregulation of IPSCs after AEA bath application compared to AEA treatment alone in any of the treatment conditions ($n = 7$, Figure 6b, c; $n = 5$, Figure 6b′, c′; $n = 10$, Figure 6b″), except for a significant AEA + Tat effect on the mean amplitude of sIPSCs in the presence of AM630 compared to control (paired t-test, $n = 10$, $p < 0.05$, Figure 6c″). For mIPSCs, the representative traces for control, AEA and AEA + Tat are shown in Figure 6d. As demonstrated with WIN55,212-2, AEA reduced the mean frequency of mIPSC (from 2.10 ± 0.51 Hz to 1.74 ± 0.51 Hz, paired t-test, $n = 8$, $p < 0.05$, Figure 6e), which was significantly blocked by rimonabant ($n = 5$, Figure 6e′) but not by AM630 ($n = 11$, e″). Further, no AEA and AEA + Tat effects were noted on the mean amplitude of mIPSCs in the absence or presence of rimonabant ($n = 8$, Figure 6f and $n = 5$, Figure 6f′, respectively). When PFC slices were pretreated with AM630 a significant downregulation of the mean amplitude of mIPSCs was noted for AEA + Tat compared to AM630 alone ($n = 11$, paired t-tests, $p < 0.05$, Figure 5f″). Thus, AEA produced a significant decrease in the mean frequency of mIPSCs and sIPSCs, which was significantly blocked by rimonabant and not further downregulated by Tat, suggesting again the decrease of GABA release by Tat was occluded by AEA, probably via a CB_1R-mediated mechanism.

Effects of Tat are blocked by CB_1R antagonist rimonabant and extracellular calcium

To understand the mechanisms by which Tat (10 nM) decreased GABAergic synaptic neurotransmission assessed by mIPSCs, we examined the involvement of rimonabant (Figure 7a), AM360 (Figure 7b), extracellular calcium (Figure 7c) and calcium channels (Figure 7d). Pretreatment with the CB_1R antagonist rimonabant (1 μM) prevented the Tat-

induced effect on the mIPSCs reported in Figure 3, with no effects on the mean frequency or the mean amplitude ($n = 8$, Figure 7a). Pretreatment with the CB_2R antagonist AM630 (1 μM) did not block the Tat-induced effects on the frequency of mIPSCs (from 2.30 ± 0.61 Hz to 2.04 ± 0.55 Hz, $n = 9$, paired t-test, $p < 0.05$, Figure 7b) but on the mean amplitude of mIPSCs ($n = 9$, Figure 7b). Removing extracellular calcium from the aCSF decreased the overall mIPSCs frequency (from 2.76 ± 0.52 Hz to 1.87 ± 0.38 Hz, $n = 7$, paired t-test, $p < 0.05$, Figure 7c) and amplitude (from 33.2 ± 2.1 pA to 30.7 ± 1.9 pA, $n = 7$, paired t-test, $p < 0.05$, Figure 7c), indicating the involvement of external calcium in GABAergic neurotransmission. More importantly, in the absence of external calcium, no significant Tat effect was noted on mIPSCs frequency and amplitude compared to zero extracellular calcium alone ($n = 7$, Figure 7c). Thus, the significant downregulation of action potential-independent GABA release (mIPSCs) by Tat was abolished when no external calcium was present in the aCSF. No effects were noted for the mean frequency or amplitude of sIPSCs (data not shown). Similarly, $CdCl_2$ (200 μM), a blocker of voltage-gated calcium currents, significantly downregulated mIPSCs compared to control, in mIPSCs frequency (from 3.21 ± 1.02 Hz to 2.42 ± 0.83 Hz, $n = 6$, paired t-test, $p < 0.05$, Figure 7d) and mIPSCs amplitude (from 28.2 ± 4.0 pA to 23.6 ± 3.3 pA, $n = 6$, paired t-test, $p < 0.05$, Figure 7d). Interestingly, whereas no significant Tat effect on the frequency of mIPSCs was noted in the presence of $CdCl_2$ ($n = 6$, Figure 7d), Tat induced a significant decrease in the amplitude of mIPSCs (from 23.6 ± 3.3 pA to 20.2 ± 1.8 pA, $n = 6$, paired t-test, $p < 0.05$, Figure 7d), indicating that other channels and receptors that are involved in Ca^{2+} influx contribute to Tat-induced effects on GABAergic neurotransmission postsynaptically. No effects were noted for the mean frequency or amplitude of sIPSCs (data not shown). Thus, the Tat-induced decrease in action potential-independent GABA release was abolished in the presence of CB_1R antagonist rimonabant but not CB_2R antagonist AM630, indicating the effects of Tat alone appear to be mediated via the CB_1R-related pathway. Further, Tat effects were abolished in the absence of extracellular calcium and partially when blocking voltage-gated calcium channels, suggesting extracellular calcium is necessary for the Tat-induced decrease in action potential-independent GABA release.

Discussion

In the present study, we used whole-cell patch-clamp recordings of acute mouse PFC slices to examine the effects of Tat and cannabinoids on GABAergic neurotransmission. This is one of the first studies to demonstrate that Tat effects on GABA release are mediated via CB_1R- but not CB_2R-related mechanism and involves the influx of extracellular calcium, partially via voltage-dependent calcium channels. Cannabinoids, WIN55,212-2 and AEA, occlude the Tat-induced decreases in GABA release as they also acted via a CB_1R-related mechanism. Based on the finding of the present study, understanding the effects of cannabinoids on GABAergic neurotransmission in the context of neuroAIDS may be an important consideration in the treatment of HAND and other diseases in which cognitive deficits occur.

Tat decreases GABAergic neurotransmission in pyramidal neurons via an action potential-independent mechanism that is mediated via CB_1Rs and involves extracellular calcium

GABA and glutamate are the most abundant neurotransmitters in the brain, and the balanced activation of inhibitory and excitatory functions is vital to maintaining the equilibrium of neuronal networks that remain under endocannabinoid modulation (Busquets-Garcia et al., 2015). Multiple studies have demonstrated that Tat mediates excitotoxic effects through the glutamatergic system (Nath et al., 1996; Haughey et al., 2001; Song et al., 2003; Fitting et al., 2014), but its effects on the GABAergic inhibitory system are not well known. Evidence from clinical studies demonstrated the involvement of the GABAergic inhibitory system in neuroAIDS, with its downregulation in HIV-1 positive individuals specifically in the frontal neocortex (Gelman et al., 2012). Downregulation of neocortical GABAergic circuits is a recognized feature in many subjects with frontal lobe dysfunction phenotypically similar to HAND. Schizophrenia (Benes and Berretta, 2001; Markram et al., 2004; Hashimoto et al., 2008), depression and anxiety (Benes and Berretta, 2001; Sequeira et al., 2009; Sibille et al., 2011) and substance abuse disorders (Ke et al., 2004) have been shown to present similar changes in GABAergic function. The lack of GABAergic inhibitory control leads to heightened excitatory output from the frontal neocortex (Markram et al., 2004; Tepper et al., 2004), which agrees with some electroencephalographic recordings made in patients with HIV/AIDS (Baldeweg and Gruzelier, 1997). Further, a recent study using Tat transgenic mice indicated that HIV-1 Tat expression in the brain as well as acute Tat application *in vitro* generated a latent excitatory state, with increased stimulus-evoked glutamate exocytosis in the cortex and hippocampus while GABA exocytosis was decreased in the cortex (Zucchini et al., 2013). The Tat-induced decrease in GABAergic neurotransmission is supported by the findings in our present study and indicates to be CB_1R-mediated and dependent on extracellular calcium, partially involving voltage-gated calcium channels. Whereas CB_1R antagonist rimonabant prevented the Tat-induced decrease in GABA release, AM630, a CB_2R antagonist, failed to block the Tat-induced effects on GABA neurotransmission. Tat could affect CB_1Rs presynaptically as GABA release can be inhibited via the well known CB_1R-mediated retrograde synaptic signaling mechanism (Kano et al., 2009; Bellocchio et al., 2010; Kovacs et al., 2012; Ohno-Shosaku and Kano, 2014; Lee et al., 2015). Previous studies have demonstrated that Tat induces loss of presynaptic terminals on hippocampal neurons in culture (Shin and Thayer, 2013). Further, the sensitivity of GABA release depending on extracellular calcium with the contribution of different voltage-gated calcium channel subtypes has been demonstrated before (Alamilla and Gillespie, 2013). Tat has been shown to cause an initial transient increase in intracellular calcium through inositol 1,4,5-trisphosphate (IP_3)-dependent calcium release (Haughey et al., 1999) as well as ryanodine-regulated calcium stores (Fitting et al., 2014) with a prolonged secondary increase due to calcium ion (Ca^{2+})-influx through plasma membrane/calcium channels that is dependent on an NMDA receptor (Haughey et al., 1999; Self et al., 2004; Chami et al., 2006). It should be noted, that in contrast to our findings a previous cortical neuron culture study demonstrated that $Tat_{30–86}$ increased presynaptic transmitter release, with increasing the frequency and amplitude of mIPSCs in target neurons by 57% and 36%, respectively (Brailoiu et al., 2008). However, this finding could be explained by the age of the cell culture (5–10 days *in vitro* (DIV)), as the change in GABAergic synaptic transmission to the inhibitory action of GABA has been shown to end in cortical neuron cultures at DIV 17 (Baltz et al., 2010).

Interestingly, it has been demonstrated that specific synaptic proteins associated with inhibitory synapses are downregulated by Tat, such as synaptotagmin 2 (Syt2) in a Tat transgenic mouse model (Fitting et al., 2013), whereas gephyrin has been shown to be upregulated in the presence of Tat (Fitting et al., 2013; Hargus and Thayer, 2013). Thus, depending on the inhibitory synaptic input and the location of recording, GABAergic neurotransmission and GABA release might be differently affected. Layer 2/3 of the mPFC, the location of our recordings, is known to receive a dense inhibitory synaptic input from different interneurons including parvalbumin-containing fast-spiking, somatostatin-containing, and neurogliaform interneurons, to provide control of neuronal excitability (Olah et al., 2009; Petersen and Crochet, 2013). A study on the hippocampus has demonstrated that neurons expressing parvalbumin in the pyramidal layer and neurons expressing somatostatin in stratum oriens might be selectively vulnerable to Tat (unpublished data).

Our results provide direct evidence that Tat concentration-dependently decreases inhibitory transmitter release in layer 2/3 of the mPFC with the involvement of extracellular calcium that is partially regulated via voltage-gated calcium channels. Additionally, the observation that Tat alters the mIPSCs, but not sIPSCs, is consistent with previous reports (Brailoiu et al., 2008) and indicates that Tat alters action potential-independent release of GABA from transmitter vesicles (Edwards et al., 1990; Shao and Dudek, 2005). As the frequency and amplitude of mIPSCs was reduced after Tat treatment, the decrease in GABAergic release could be explained by the inhibition of the vesicle release machinery in the presynaptic axon terminal (presynaptic inhibition) and a decrease of postsynaptic receptors due to a reduction in mIPSC amplitude (postsynaptic inhibition). A significant downregulation of pre- and post-synaptic GABAergic inhibitory systems was reported selectively in the frontal neocortex of HIV-1 positive patients with neurocognitive impairments (Gelman et al., 2012). Thus, as neuronal excitability and synaptic plasticity at excitatory synapses are critically dependent on the level of inhibition, changes of inhibitory synaptic efficacy by Tat may have great impact on neuronal function and toxicity and need to be considered in the future.

Synthetic cannabinoid WIN55,212-2 and endocannabinoid AEA decrease GABAergic neurotransmission in PFC pyramidal neurons via a CB_1R-mediated mechanism and without any further downregulation by Tat

Multiple studies have investigated the effects of cannabinoids on GABAergic synaptic transmission (Bellocchio et al., 2010; Kovacs et al., 2012; Ohno-Shosaku and Kano, 2014; Lee et al., 2015). It is now well accepted that endocannabinoids are released from postsynaptic neurons and cause transient and long-lasting reduction of neurotransmitter release (Gerdeman and Lovinger, 2001; Huang et al., 2001; Kano et al., 2009). As reported in the present study it also has been shown previously that WIN55,212-2 decreases the frequency of mIPSCs recorded in the presence of TTX, but does not change mIPSCs amplitude, indicating that the neurotransmission is inhibited presynaptically (Vaughan et al., 1999; Takahashi and Linden, 2000; Trettel and Levine, 2002; Chevaleyre et al., 2007; Chiu et al., 2010; Kovacs et al., 2012). Similarly, in the present study the exogenous application of AEA not only decreased mIPSC frequency without changing mIPSC amplitude but also decreased sIPSCs frequency. It has been shown previously that AEA affects sIPSC frequency (Adermark and Lovinger, 2007). The reduced mIPSC frequency by AEA might

have resulted from a decreased transmitter-release probability after AEA treatment, as a decrease in sIPSC frequency was noted. The reduction in frequency of mIPSCs suggests again presynaptic inhibition with two mechanisms that could potentially contribute to this result: fewer GABAergic presynaptic terminals on the pyramidal neurons and/or decreased release probability in those terminals. Further experiments would be required to distinguish between these two mechanisms.

The AEA-induced decrease in mIPSC and sIPSC frequency was blocked by the selective CB_1R antagonist rimonabant, but not the CB_2R antagonist AM630, demonstrating CB_1R mediation, a finding consistent with other studies (Trettel and Levine, 2002; Bodor et al., 2005; Hill et al., 2007; Galarreta et al., 2008; Chiu et al., 2010). Interestingly, rimonabant but not AM630 blocked the effects of WIN55,212-2, which is known to be not very specific to CB_1R-mediated mechanisms (Hofmann et al., 2011). Previous literature has demonstrated that WIN55,212-2 can act via non-CB_1/CB_2-mediated mechanisms by activating $G_{i/o}$ proteins (Hajos et al., 2001; Fung et al., 2015). Even though AM630 failed to block the effects of WIN55,212-2 it should be noted that it induced a decrease in the mean amplitude of mIPSCs, which otherwise is not affected by WIN55,212-2 or AM630 alone. Thus, some CB_2R-related mechanism might be involved postsynaptically or might be related to glial activity (Kim et al., 2011; Hu et al., 2013). Interestingly, WIN55,212-2 or AEA bath application following or preceding Tat treatment occluded the Tat-induced decrease in GABA release, suggesting that WIN55,212-2 and/or AEA and Tat might use similar pathways to decrease GABAergic neurotransmission, including a CB_1R-mediated mechanism. For example, several mechanisms have been offered to explain CB_1R-mediated suppression of neurotransmitter release, including inhibition of voltage-gated calcium channels, activation of a number of potassium channels, and inhibition of release machinery (Schlicker and Kathmann, 2001; Chevaleyre et al., 2006). As Tat effects were abolished for mIPSCs frequency, but not mIPSCs amplitude when blocking the voltage-gated calcium channels with $CdCl_2$, it appears that the voltage-gated calcium channels could represent a presynaptic mechanism of Tat to inhibit GABA release. Nevertheless, Tat significantly reduced mIPSC amplitude in contrast to the endocannabinoids, indicating that Tat also affects postsynaptic inhibition by potentially altering number of postsynaptic receptors (Hargus and Thayer, 2013). Interestingly, the Tat-induced decrease in mean amplitude of mIPSCs was blocked when PFC slices were pretreated with WIN55,212-2 or AEA, indicating some indirect mechanisms by which endocannabinoids can affect Tat-induced postsynaptic inhibition.

Conclusion

The present study demonstrates that Tat inhibits GABAergic neurotransmission in the mouse mPFC (layer2/3) and that endocannabinoids occlude the Tat-induced suppression of GABA release by acting on CB_1Rs. The interaction of Tat and endocannabinoids on inhibitory synaptic transmission in the PFC may partially contribute to the protective effects elicited by endocannabinoids that have been reported in different disease models (Zhuang et al., 2005; Liu et al., 2009; Kim et al., 2011; Hu et al., 2013; Kokona and Thermos, 2015), but requires further investigation in the context of neuroAIDS/HIV-1 Tat toxicity.

Acknowledgments

Funding

This study was funded by the National Institute on Drug Abuse (NIDA R00 DA033878, T32 DA007244, R01 DA032933, K05 DA021696, R01 DA011322).

References

Adermark L, Lovinger DM. Retrograde endocannabinoid signaling at striatal synapses requires a regulated postsynaptic release step. Proc Natl Acad Sci U S A. 2007; 104:20564–20569. [PubMed: 18077376]

Aksenov MY, Aksenova MV, Mactutus CF, Booze RM. D_1/NMDA receptors and concurrent methamphetamine + HIV-1 Tat neurotoxicity. J Neuroimmune Pharmacol. 2012; 7:599–608. [PubMed: 22552781]

Alamilla J, Gillespie DC. Maturation of calcium-dependent GABA, glycine, and glutamate release in the glycinergic MNTB-LSO pathway. PLoS One. 2013; 8:e75688. [PubMed: 24069436]

Auclair N, Otani S, Soubrie P, Crepel F. Cannabinoids modulate synaptic strength and plasticity at glutamatergic synapses of rat prefrontal cortex pyramidal neurons. J Neurophysiol. 2000; 83:3287–3293. [PubMed: 10848548]

Avraham HK, Jiang S, Fu Y, Rockenstein E, Makriyannis A, Zvonok A, Masliah E, Avraham S. The cannabinoid CB(2) receptor agonist AM1241 enhances neurogenesis in GFAP/Gp120 transgenic mice displaying deficits in neurogenesis. Br J Pharmacol. 2014; 171:468–479. [PubMed: 24148086]

Baldeweg T, Gruzelier JH. Alpha EEG activity and subcortical pathology in HIV infection. International journal of psychophysiology: official journal of the International Organization of Psychophysiology. 1997; 26:431–442. [PubMed: 9203019]

Baltz T, de Lima AD, Voigt T. Contribution of GABAergic interneurons to the development of spontaneous activity patterns in cultured neocortical networks. Frontiers in cellular neuroscience. 2010; 4:15. [PubMed: 20617185]

Bellocchio L, Lafenetre P, Cannich A, Cota D, Puente N, Grandes P, Chaouloff F, Piazza PV, Marsicano G. Bimodal control of stimulated food intake by the endocannabinoid system. Nat Neurosci. 2010; 13:281–283. [PubMed: 20139974]

Benes FM, Berretta S. GABAergic interneurons: implications for understanding schizophrenia and bipolar disorder. Neuropsychopharmacology. 2001; 25:1–27. [PubMed: 11377916]

Berger JR, Arendt G. HIV dementia: the role of the basal ganglia and dopaminergic systems. J Psychopharmacol. 2000; 14:214–221. [PubMed: 11106299]

Bertrand SJ, Mactutus CF, Aksenova MV, Espensen-Sturges TD, Booze RM. Synaptodendritic recovery following HIV Tat exposure: neurorestoration by phytoestrogens. J Neurochem. 2014; 128:140–151. [PubMed: 23875777]

Bodor AL, Katona I, Nyiri G, Mackie K, Ledent C, Hajos N, Freund TF. Endocannabinoid signaling in rat somatosensory cortex: laminar differences and involvement of specific interneuron types. J Neurosci. 2005; 25:6845–6856. [PubMed: 16033894]

Brailoiu GC, Brailoiu E, Chang JK, Dun NJ. Excitatory effects of human immunodeficiency virus 1 Tat on cultured rat cerebral cortical neurons. Neuroscience. 2008; 151:701–710. [PubMed: 18164555]

Busquets-Garcia A, Desprez T, Metna-Laurent M, Bellocchio L, Marsicano G, Soria-Gomez E. Dissecting the cannabinergic control of behavior: The where matters. Bioessays. 2015; 37:1215–1225. [PubMed: 26260530]

Carey AN, Sypek EI, Singh HD, Kaufman MJ, McLaughlin JP. Expression of HIV-Tat protein is associated with learning and memory deficits in the mouse. Behav Brain Res. 2012; 229:48–56. [PubMed: 22197678]

Chami M, Oules B, Paterlini-Brechot P. Cytobiological consequences of calcium-signaling alterations induced by human viral proteins. Biochim Biophys Acta. 2006; 1763:1344–1362. [PubMed: 17059849]

Chen CY, Bonham AC, Dean C, Hopp FA, Hillard CJ, Seagard JL. Retrograde release of endocannabinoids inhibits presynaptic GABA release to second-order baroreceptive neurons in NTS. Auton Neurosci. 2010; 158:44–50. [PubMed: 20580326]

Chevaleyre V, Takahashi KA, Castillo PE. Endocannabinoid-mediated synaptic plasticity in the CNS. Annu Rev Neurosci. 2006; 29:37–76. [PubMed: 16776579]

Chevaleyre V, Heifets BD, Kaeser PS, Sudhof TC, Castillo PE. Endocannabinoid-mediated long-term plasticity requires cAMP/PKA signaling and RIM1alpha. Neuron. 2007; 54:801–812. [PubMed: 17553427]

Chiu CQ, Puente N, Grandes P, Castillo PE. Dopaminergic modulation of endocannabinoid-mediated plasticity at GABAergic synapses in the prefrontal cortex. J Neurosci. 2010; 30:7236–7248. [PubMed: 20505090]

Di Marzo V, Stella N, Zimmer A. Endocannabinoid signalling and the deteriorating brain. Nat Rev Neurosci. 2015; 16:30–42. [PubMed: 25524120]

Edwards FA, Konnerth A, Sakmann B. Quantal analysis of inhibitory synaptic transmission in the dentate gyrus of rat hippocampal slices: a patch-clamp study. J Physiol. 1990; 430:213–249. [PubMed: 1707966]

Ellis R, Langford D, Masliah E. HIV and antiretroviral therapy in the brain: neuronal injury and repair. Nat Rev Neurosci. 2007; 8:33–44. [PubMed: 17180161]

Ernst T, Jiang CS, Nakama H, Buchthal S, Chang L. Lower brain glutamate is associated with cognitive deficits in HIV patients: a new mechanism for HIV-associated neurocognitive disorder. J Magn Reson Imaging. 2010; 32:1045–1053. [PubMed: 21031507]

Ferrarese C, Aliprandi A, Tremolizzo L, Stanzani L, De Micheli A, Dolara A, Frattola L. Increased glutamate in CSF and plasma of patients with HIV dementia. Neurology. 2001; 57:671–675. [PubMed: 11524477]

Fitting S, Knapp PE, Zou S, Marks WD, Bowers MS, Akbarali HI, Hauser KF. Interactive HIV-1 Tat and morphine-induced synaptodendritic injury is triggered through focal disruptions in Na^+ influx, mitochondrial instability, and Ca^{2+} overload. J Neurosci. 2014; 34:12850–12864. [PubMed: 25232120]

Fitting S, Xu R, Bull C, Buch SK, El-Hage N, Nath A, Knapp PE, Hauser KF. Interactive comorbidity between opioid drug abuse and HIV-1 Tat: chronic exposure augments spine loss and sublethal dendritic pathology in striatal neurons. Am J Pathol. 2010; 177:1397–1410. [PubMed: 20651230]

Fitting S, Ignatowska-Jankowska BM, Bull C, Skoff RP, Lichtman AH, Wise LE, Fox MA, Su J, Medina AE, Krahe TE, Knapp PE, Guido W, Hauser KF. Synaptic dysfunction in the hippocampus accompanies learning and memory deficits in human immunodeficiency virus type-1 Tat transgenic mice. Biol Psychiatry. 2013; 73:443–453. [PubMed: 23218253]

Fung S, Cherry AE, Xu C, Stella N. Alkylindole-sensitive receptors modulate microglial cell migration and proliferation. Glia. 2015; 63:1797–1808. [PubMed: 25914169]

Galarreta M, Erdelyi F, Szabo G, Hestrin S. Cannabinoid sensitivity and synaptic properties of 2 GABAergic networks in the neocortex. Cereb Cortex. 2008; 18:2296–2305. [PubMed: 18203691]

Gelman BB, Spencer JA, Holzer CE 3rd, Soukup VM. Abnormal striatal dopaminergic synapses in National NeuroAIDS Tissue Consortium subjects with HIV encephalitis. J Neuroimmune Pharmacol. 2006; 1:410–420. [PubMed: 18040813]

Gelman BB, Chen T, Lisinicchia JG, Soukup VM, Carmical JR, Starkey JM, Masliah E, Commins DL, Brandt D, Grant I, Singer EJ, Levine AJ, Miller J, Winkler JM, Fox HS, Luxon BA, Morgello S, National Neuro ATC. The National NeuroAIDS Tissue Consortium brain gene array: two types of HIV-associated neurocognitive impairment. PLoS One. 2012; 7:e46178. [PubMed: 23049970]

Gerdeman G, Lovinger DM. CB1 cannabinoid receptor inhibits synaptic release of glutamate in rat dorsolateral striatum. J Neurophysiol. 2001; 85:468–471. [PubMed: 11152748]

Grant I, Cahn BR. Cannabis and endocannabinoid modulators: Therapeutic promises and challenges. Clin Neurosci Res. 2005; 5:185–199. [PubMed: 18806886]

Hahn YK, Podhaizer EM, Farris SP, Miles MF, Hauser KF, Knapp PE. Effects of chronic HIV-1 Tat exposure in the CNS: heightened vulnerability of males versus females to changes in cell numbers, synaptic integrity, and behavior. Brain Struct Funct. 2013; 220:605–623. [PubMed: 24352707]

Hajos N, Ledent C, Freund TF. Novel cannabinoid-sensitive receptor mediates inhibition of glutamatergic synaptic transmission in the hippocampus. Neuroscience. 2001; 106:1–4. [PubMed: 11564411]

Hargus NJ, Thayer SA. Human immunodeficiency virus-1 Tat protein increases the number of inhibitory synapses between hippocampal neurons in culture. J Neurosci. 2013; 33:17908–17920. [PubMed: 24198379]

Harkany T, Mackie K, Doherty P. Wiring and firing neuronal networks: endocannabinoids take center stage. Curr Opin Neurobiol. 2008; 18:338–345. [PubMed: 18801434]

Hashimoto T, Bazmi HH, Mirnics K, Wu Q, Sampson AR, Lewis DA. Conserved regional patterns of GABA-related transcript expression in the neocortex of subjects with schizophrenia. Am J Psychiatry. 2008; 165:479–489. [PubMed: 18281411]

Haughey NJ, Mattson MP. Calcium dysregulation and neuronal apoptosis by the HIV-1 proteins Tat and gp120. J Acquir Immune Defic Syndr. 2002; 31(Suppl 2):S55–61. [PubMed: 12394783]

Haughey NJ, Holden CP, Nath A, Geiger JD. Involvement of inositol 1,4,5-trisphosphate-regulated stores of intracellular calcium in calcium dysregulation and neuron cell death caused by HIV-1 protein tat. J Neurochem. 1999; 73:1363–1374. [PubMed: 10501179]

Haughey NJ, Nath A, Mattson MP, Slevin JT, Geiger JD. HIV-1 Tat through phosphorylation of NMDA receptors potentiates glutamate excitotoxicity. J Neurochem. 2001; 78:457–467. [PubMed: 11483648]

Heaton RK, et al. HIV-associated neurocognitive disorders before and during the era of combination antiretroviral therapy: differences in rates, nature, and predictors. J Neurovirol. 2011; 17:3–16. [PubMed: 21174240]

Higgins A, Yuan S, Wang Y, Burrell BD. Differential modulation of nociceptive versus non-nociceptive synapses by endocannabinoids. Mol Pain. 2013; 9:26. [PubMed: 23725095]

Hill EL, Gallopin T, Ferezou I, Cauli B, Rossier J, Schweitzer P, Lambolez B. Functional CB1 receptors are broadly expressed in neocortical GABAergic and glutamatergic neurons. J Neurophysiol. 2007; 97:2580–2589. [PubMed: 17267760]

Hoffman AF, Lupica CR. Mechanisms of cannabinoid inhibition of GABA(A) synaptic transmission in the hippocampus. J Neurosci. 2000; 20:2470–2479. [PubMed: 10729327]

Hofmann ME, Bhatia C, Frazier CJ. Cannabinoid receptor agonists potentiate action potential-independent release of GABA in the dentate gyrus through a CB1 receptor-independent mechanism. J Physiol. 2011; 589:3801–3821. [PubMed: 21646412]

Howlett AC, Blume LC, Dalton GD. CB(1) cannabinoid receptors and their associated proteins. Curr Med Chem. 2010; 17:1382–1393. [PubMed: 20166926]

Hu S, Sheng WS, Rock RB. CB2 receptor agonists protect human dopaminergic neurons against damage from HIV-1 gp120. PLoS One. 2013; 8:e77577. [PubMed: 24147028]

Huang CC, Lo SW, Hsu KS. Presynaptic mechanisms underlying cannabinoid inhibition of excitatory synaptic transmission in rat striatal neurons. J Physiol. 2001; 532:731–748. [PubMed: 11313442]

Kano M. Control of synaptic function by endocannabinoid-mediated retrograde signaling. Proc Jpn Acad Ser B Phys Biol Sci. 2014; 90:235–250.

Kano M, Ohno-Shosaku T, Hashimotodani Y, Uchigashima M, Watanabe M. Endocannabinoid-mediated control of synaptic transmission. Physiol Rev. 2009; 89:309–380. [PubMed: 19126760]

Ke Y, Streeter CC, Nassar LE, Sarid-Segal O, Hennen J, Yurgelun-Todd DA, Awad LA, Rendall MJ, Gruber SA, Nason A, Mudrick MJ, Blank SR, Meyer AA, Knapp C, Ciraulo DA, Renshaw PF. Frontal lobe GABA levels in cocaine dependence: a two-dimensional, J-resolved magnetic resonance spectroscopy study. Psychiatry research. 2004; 130:283–293. [PubMed: 15135161]

Kim HJ, Martemyanov KA, Thayer SA. Human immunodeficiency virus protein Tat induces synapse loss via a reversible process that is distinct from cell death. J Neurosci. 2008; 28:12604–12613. [PubMed: 19036954]

Kim HJ, Shin AH, Thayer SA. Activation of cannabinoid type 2 receptors inhibits HIV-1 envelope glycoprotein gp120-induced synapse loss. Mol Pharmacol. 2011; 80:357–366. [PubMed: 21670103]

Kokona D, Thermos K. Synthetic and endogenous cannabinoids protect retinal neurons from AMPA excitotoxicity in vivo, via activation of CB1 receptors: Involvement of PI3K/Akt and MEK/ERK signaling pathways. Experimental eye research. 2015; 136:45–58. [PubMed: 25989217]

Kovacs FE, Knop T, Urbanski MJ, Freiman I, Freiman TM, Feuerstein TJ, Zentner J, Szabo B. Exogenous and endogenous cannabinoids suppress inhibitory neurotransmission in the human neocortex. Neuropsychopharmacology. 2012; 37:1104–1114. [PubMed: 22048459]

Kruman II, Nath A, Mattson MP. HIV-1 protein Tat induces apoptosis of hippocampal neurons by a mechanism involving caspase activation, calcium overload, and oxidative stress. Exp Neurol. 1998; 154:276–288. [PubMed: 9878167]

Lee SH, Ledri M, Toth B, Marchionni I, Henstridge CM, Dudok B, Kenesei K, Barna L, Szabo SI, Renkecz T, Oberoi M, Watanabe M, Limoli CL, Horvai G, Soltesz I, Katona I. Multiple Forms of Endocannabinoid and Endovanilloid Signaling Regulate the Tonic Control of GABA Release. J Neurosci. 2015; 35:10039–10057. [PubMed: 26157003]

Li W, Huang Y, Reid R, Steiner J, Malpica-Llanos T, Darden TA, Shankar SK, Mahadevan A, Satishchandra P, Nath A. NMDA receptor activation by HIV-Tat protein is clade dependent. J Neurosci. 2008; 28:12190–12198. [PubMed: 19020013]

Liu Q, Bhat M, Bowen WD, Cheng J. Signaling pathways from cannabinoid receptor-1 activation to inhibition of N-methyl-D-aspartic acid mediated calcium influx and neurotoxicity in dorsal root ganglion neurons. J Pharmacol Exp Ther. 2009; 331:1062–1070. [PubMed: 19752241]

Longordo F, Feligioni M, Chiaramonte G, Sbaffi PF, Raiteri M, Pittaluga A. The human immunodeficiency virus-1 protein transactivator of transcription up-regulates N-methyl-D-aspartate receptor function by acting at metabotropic glutamate receptor 1 receptors coexisting on human and rat brain noradrenergic neurones. J Pharmacol Exp Ther. 2006; 317:1097–1105. [PubMed: 16489129]

Magnuson DS, Knudsen BE, Geiger JD, Brownstone RM, Nath A. Human immunodeficiency virus type 1 tat activates non-N-methyl-D-aspartate excitatory amino acid receptors and causes neurotoxicity. Ann Neurol. 1995; 37:373–380. [PubMed: 7695237]

Markram H, Toledo-Rodriguez M, Wang Y, Gupta A, Silberberg G, Wu C. Interneurons of the neocortical inhibitory system. Nat Rev Neurosci. 2004; 5:793–807. [PubMed: 15378039]

Maroof N, Pardon MC, Kendall DA. Endocannabinoid signalling in Alzheimer's disease. Biochem Soc Trans. 2013; 41:1583–1587. [PubMed: 24256258]

Masliah E, Heaton RK, Marcotte TD, Ellis RJ, Wiley CA, Mallory M, Achim CL, McCutchan JA, Nelson JA, Atkinson JH, Grant I. Dendritic injury is a pathological substrate for human immunodeficiency virus-related cognitive disorders. HNRC Group. The HIV Neurobehavioral Research Center. Ann Neurol. 1997; 42:963–972. [PubMed: 9403489]

Matsuda LA, Lolait SJ, Brownstein MJ, Young AC, Bonner TI. Structure of a cannabinoid receptor and functional expression of the cloned cDNA. Nature. 1990; 346:561–564. [PubMed: 2165569]

Moran LM, Booze RM, Mactutus CF. Time and time again: temporal processing demands implicate perceptual and gating deficits in the HIV-1 transgenic rat. J Neuroimmune Pharmacol. 2013; 8:988–997. [PubMed: 23690140]

Murray MF. Tryptophan depletion and HIV infection: a metabolic link to pathogenesis. The Lancet Infectious diseases. 2003; 3:644–652. [PubMed: 14522263]

Nath A, Psooy K, Martin C, Knudsen B, Magnuson DS, Haughey N, Geiger JD. Identification of a human immunodeficiency virus type 1 Tat epitope that is neuroexcitatory and neurotoxic. J Virol. 1996; 70:1475–1480. [PubMed: 8627665]

Nath A, Anderson C, Jones M, Maragos W, Booze R, Mactutus C, Bell J, Hauser KF, Mattson M. Neurotoxicity and dysfunction of dopaminergic systems associated with AIDS dementia. J Psychopharmacol. 2000; 14:222–227. [PubMed: 11106300]

National Research Council. Guide for the Care and Use of Laboratory Animals. 8. Washington, DC: National Academies Press; 2011.

Ohno-Shosaku T, Kano M. Endocannabinoid-mediated retrograde modulation of synaptic transmission. Curr Opin Neurobiol. 2014; 29:1–8. [PubMed: 24747340]

Olah S, Fule M, Komlosi G, Varga C, Baldi R, Barzo P, Tamas G. Regulation of cortical microcircuits by unitary GABA-mediated volume transmission. Nature. 2009; 461:1278–1281. [PubMed: 19865171]

Paris JJ, Singh HD, Carey AN, McLaughlin JP. Exposure to HIV-1 Tat in brain impairs sensorimotor gating and activates microglia in limbic and extralimbic brain regions of male mice. Behav Brain Res. 2015; 291:209–218. [PubMed: 26005128]

Perez A, Probert AW, Wang KK, Sharmeen L. Evaluation of HIV-1 Tat induced neurotoxicity in rat cortical cell culture. J Neurovirol. 2001; 7:1–10. [PubMed: 11519477]

Pertwee RG. Elevating endocannabinoid levels: pharmacological strategies and potential therapeutic applications. The Proceedings of the Nutrition Society. 2014; 73:96–105. [PubMed: 24135210]

Petersen CC, Crochet S. Synaptic computation and sensory processing in neocortical layer 2/3. Neuron. 2013; 78:28–48. [PubMed: 23583106]

Roscoe RF Jr, Mactutus CF, Booze RM. HIV-1 transgenic female rat: synaptodendritic alterations of medium spiny neurons in the nucleus accumbens. J Neuroimmune Pharmacol. 2014; 9:642–653. [PubMed: 25037595]

Ross GR, Lichtman A, Dewey WL, Akbarali HI. Evidence for the putative cannabinoid receptor (GPR55)-mediated inhibitory effects on intestinal contractility in mice. Pharmacology. 2012; 90:55–65. [PubMed: 22759743]

Schlicker E, Kathmann M. Modulation of transmitter release via presynaptic cannabinoid receptors. Trends Pharmacol Sci. 2001; 22:565–572. [PubMed: 11698100]

Schroecksnadel K, Zangerle R, Bellmann-Weiler R, Garimorth K, Weiss G, Fuchs D. Indoleamine-2, 3-dioxygenase and other interferon-gamma-mediated pathways in patients with human immunodeficiency virus infection. Curr Drug Metab. 2007; 8:225–236. [PubMed: 17430111]

Scotter EL, Abood ME, Glass M. The endocannabinoid system as a target for the treatment of neurodegenerative disease. Br J Pharmacol. 2010; 160:480–498. [PubMed: 20590559]

Self RL, Mulholland PJ, Nath A, Harris BR, Prendergast MA. The human immunodeficiency virus type-1 transcription factor Tat produces elevations in intracellular Ca^{2+} that require function of an N-methyl-D-aspartate receptor polyamine-sensitive site. Brain Res. 2004; 995:39–45. [PubMed: 14644469]

Sequeira A, Mamdani F, Ernst C, Vawter MP, Bunney WE, Lebel V, Rehal S, Klempan T, Gratton A, Benkelfat C, Rouleau GA, Mechawar N, Turecki G. Global brain gene expression analysis links glutamatergic and GABAergic alterations to suicide and major depression. PLoS One. 2009; 4:e6585. [PubMed: 19668376]

Shao LR, Dudek FE. Changes in mIPSCs and sIPSCs after kainate treatment: evidence for loss of inhibitory input to dentate granule cells and possible compensatory responses. J Neurophysiol. 2005; 94:952–960. [PubMed: 15772233]

Shin AH, Thayer SA. Human immunodeficiency virus-1 protein Tat induces excitotoxic loss of presynaptic terminals in hippocampal cultures. Mol Cell Neurosci. 2013; 54:22–29. [PubMed: 23267846]

Sibille E, Morris HM, Kota RS, Lewis DA. GABA-related transcripts in the dorsolateral prefrontal cortex in mood disorders. The international journal of neuropsychopharmacology/official scientific journal of the Collegium Internationale Neuropsychopharmacologicum. 2011; 14:721–734.

Singh IN, Goody RJ, Dean C, Ahmad NM, Lutz SE, Knapp PE, Nath A, Hauser KF. Apoptotic death of striatal neurons induced by human immunodeficiency virus-1 Tat and gp120: differential involvement of caspase-3 and endonuclease G. J Neurovirol. 2004; 10:141–151. [PubMed: 15204919]

Song L, Nath A, Geiger JD, Moore A, Hochman S. Human immunodeficiency virus type 1 Tat protein directly activates neuronal N-methyl-D-aspartate receptors at an allosteric zinc-sensitive site. J Neurovirol. 2003; 9:399–403. [PubMed: 12775422]

Takahashi KA, Linden DJ. Cannabinoid receptor modulation of synapses received by cerebellar Purkinje cells. J Neurophysiol. 2000; 83:1167–1180. [PubMed: 10712447]

Tepper JM, Koos T, Wilson CJ. GABAergic microcircuits in the neostriatum. Trends Neurosci. 2004; 27:662–669. [PubMed: 15474166]

Trettel J, Levine ES. Cannabinoids depress inhibitory synaptic inputs received by layer 2/3 pyramidal neurons of the neocortex. J Neurophysiol. 2002; 88:534–539. [PubMed: 12091577]

Tsou K, Brown S, Sanudo-Pena MC, Mackie K, Walker JM. Immunohistochemical distribution of cannabinoid CB1 receptors in the rat central nervous system. Neuroscience. 1998; 83:393–411. [PubMed: 9460749]

Vaughan CW, McGregor IS, Christie MJ. Cannabinoid receptor activation inhibits GABAergic neurotransmission in rostral ventromedial medulla neurons in vitro. Br J Pharmacol. 1999; 127:935–940. [PubMed: 10433501]

Wang GJ, Chang L, Volkow ND, Telang F, Logan J, Ernst T, Fowler JS. Decreased brain dopaminergic transporters in HIV-associated dementia patients. Brain. 2004; 127:2452–2458. [PubMed: 15319273]

Xu C, Cui C, Alkon DL. Age-dependent enhancement of inhibitory synaptic transmission in CA1 pyramidal neurons via GluR5 kainate receptors. Hippocampus. 2009; 19:706–717. [PubMed: 19123252]

Xu JY, Chen C. Endocannabinoids in synaptic plasticity and neuroprotection. Neuroscientist. 2015; 21:152–168. [PubMed: 24571856]

Yuan S, Burrell BD. Nonnociceptive afferent activity depresses nocifensive behavior and nociceptive synapses via an endocannabinoid-dependent mechanism. J Neurophysiol. 2013; 110:2607–2616. [PubMed: 24027102]

Zhuang SY, Bridges D, Grigorenko E, McCloud S, Boon A, Hampson RE, Deadwyler SA. Cannabinoids produce neuroprotection by reducing intracellular calcium release from ryanodine-sensitive stores. Neuropharmacology. 2005; 48:1086–1096. [PubMed: 15910885]

Zucchini S, Pittaluga A, Brocca-Cofano E, Summa M, Fabris M, De Michele R, Bonaccorsi A, Busatto G, Barbanti-Brodano G, Altavilla G, Verlengia G, Cifelli P, Corallini A, Caputo A, Simonato M. Increased excitability in tat-transgenic mice: role of tat in HIV-related neurological disorders. Neurobiol Dis. 2013; 55:110–119. [PubMed: 23454193]

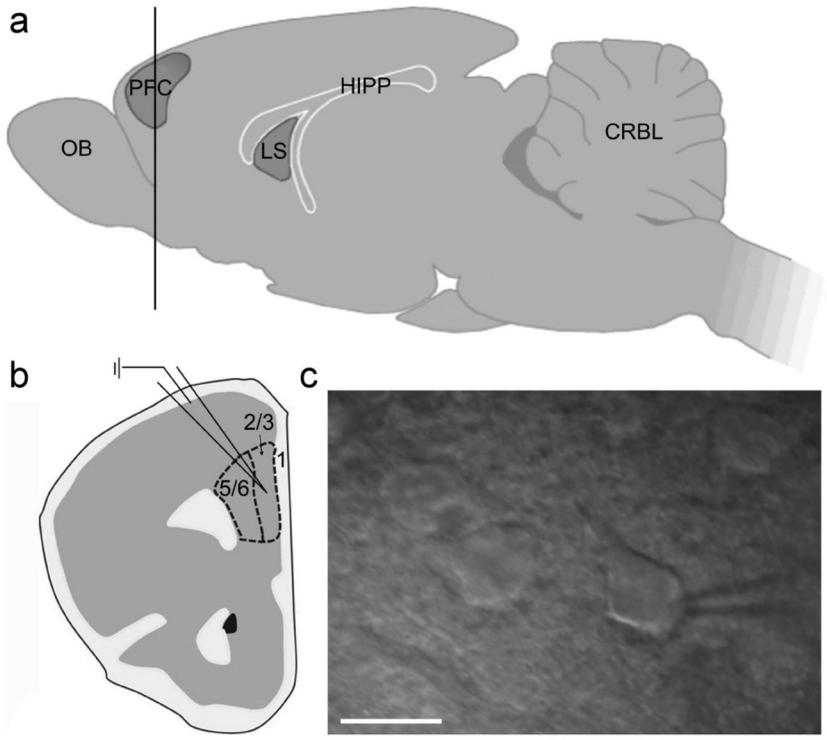

Figure 1. Electrophysiology conducted in PFC slices of postnatal day P14 – 24 mice

(a) Lateral view of the mouse brain with a coronal cut through the PFC (horizontal line). (b) Diagram of a coronal PFC slice, indicating the location of whole cell recordings conducted in layer 2/3 of the mPFC (dashed line). (c) Pyramidal neurons were identified by their triangular shape with infrared differential interference contrast and integrated Dodt gradient optics (40x). Scale bar: 20 μm. OB, olfactory bulb; PFC, prefrontal cortex; LS, lateral septum; HIPP, hippocampus; CRBL, cerebellum.

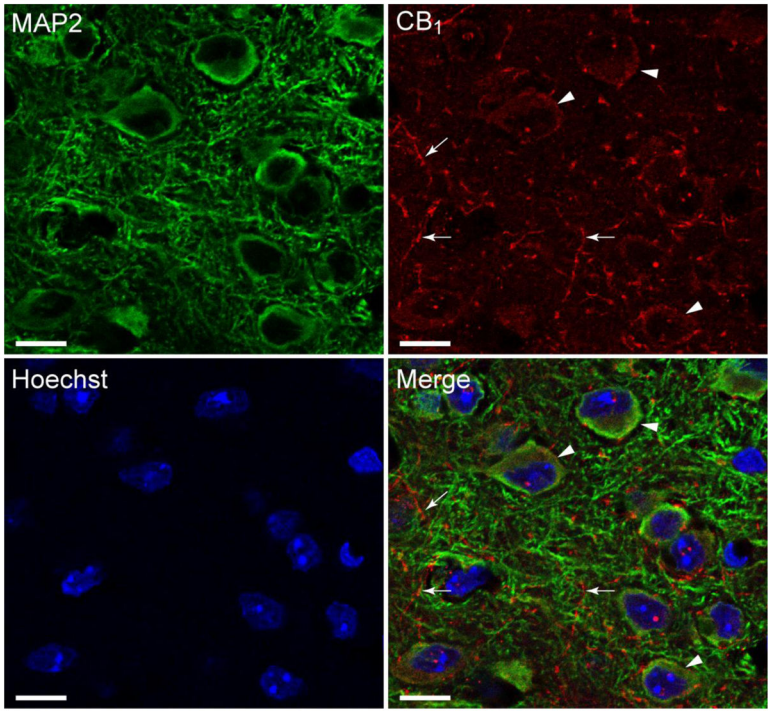

Figure 2. Pyramidal PFC neurons harbor CB_1R-like immunoreactivity

Confocal microscope images of mouse mPFC tissue of layer 2/3, immunostained and double-labeled for MAP2 (microtubule-associated protein 2, an important structural and functional component of dendrites; green), the 1-77 amino acid N-terminus CB_1R (G protein-coupled cannabinoid receptor; red), and counterstained with Hoechst 33342 (nuclear DNA label, blue). The merged image indicates that CB_1R (red) is specifically localized in the soma (arrowheads) and axons (arrows) of mPFC mouse tissue. Scale bar: 20 μm.

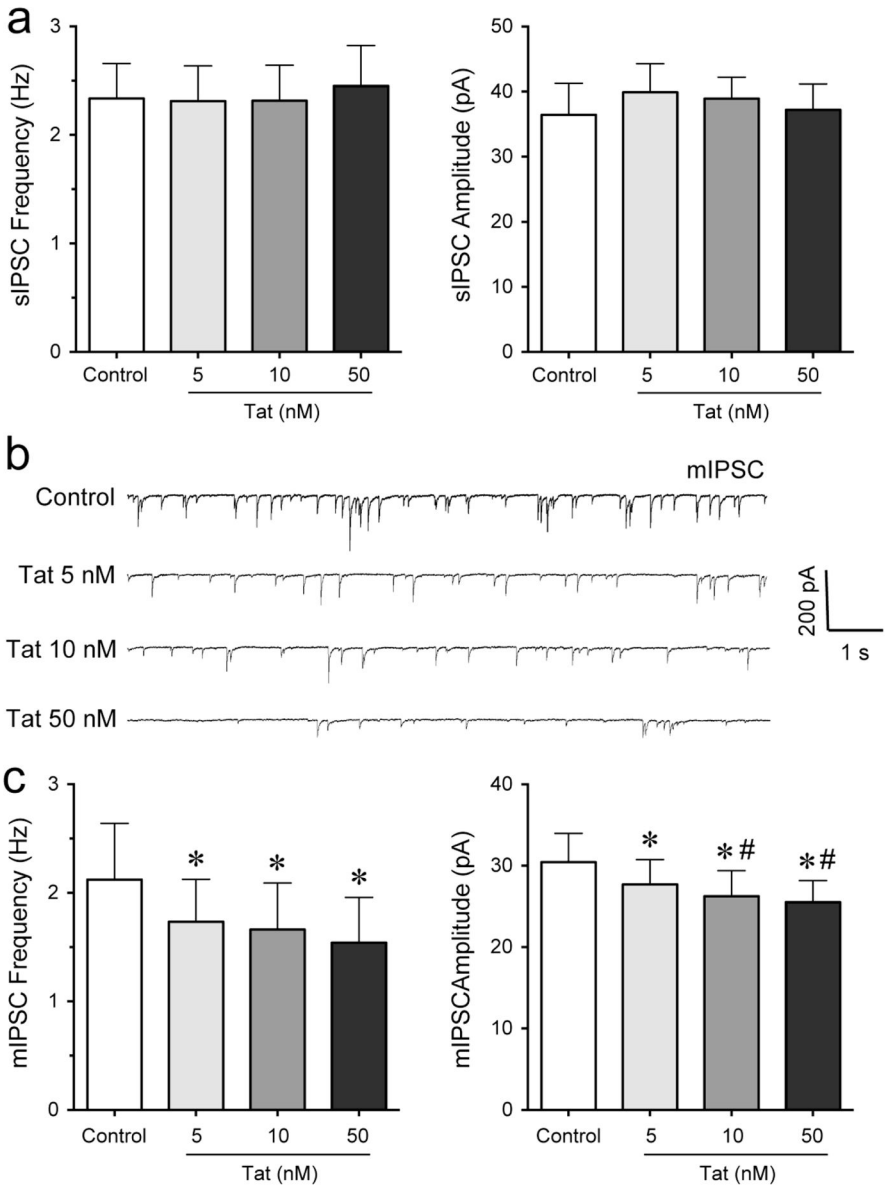

Figure 3. Tat concentration-dependently decreased the frequency and amplitude of mIPSCs but not sIPSC in PFC pyramidal neurons

(a) No significant Tat (5 – 50 nM) effects were noted on the mean frequency and amplitude of sIPSCs ($n = 6$). (b) Representative traces show mIPSCs before and after application of Tat concentrations (5 – 50 nM). (c) Different concentrations of Tat (5 – 50 nM) concentration-dependently decreased the mean frequency and amplitude of mIPSCs at 5 min following Tat application ($n = 11$). Data are mean ± SEM. Significance was assessed by paired Student *t*-tests. $^{*}p < 0.05$ vs. Control, $^{\#}p < 0.05$ vs. Tat (5 nM).

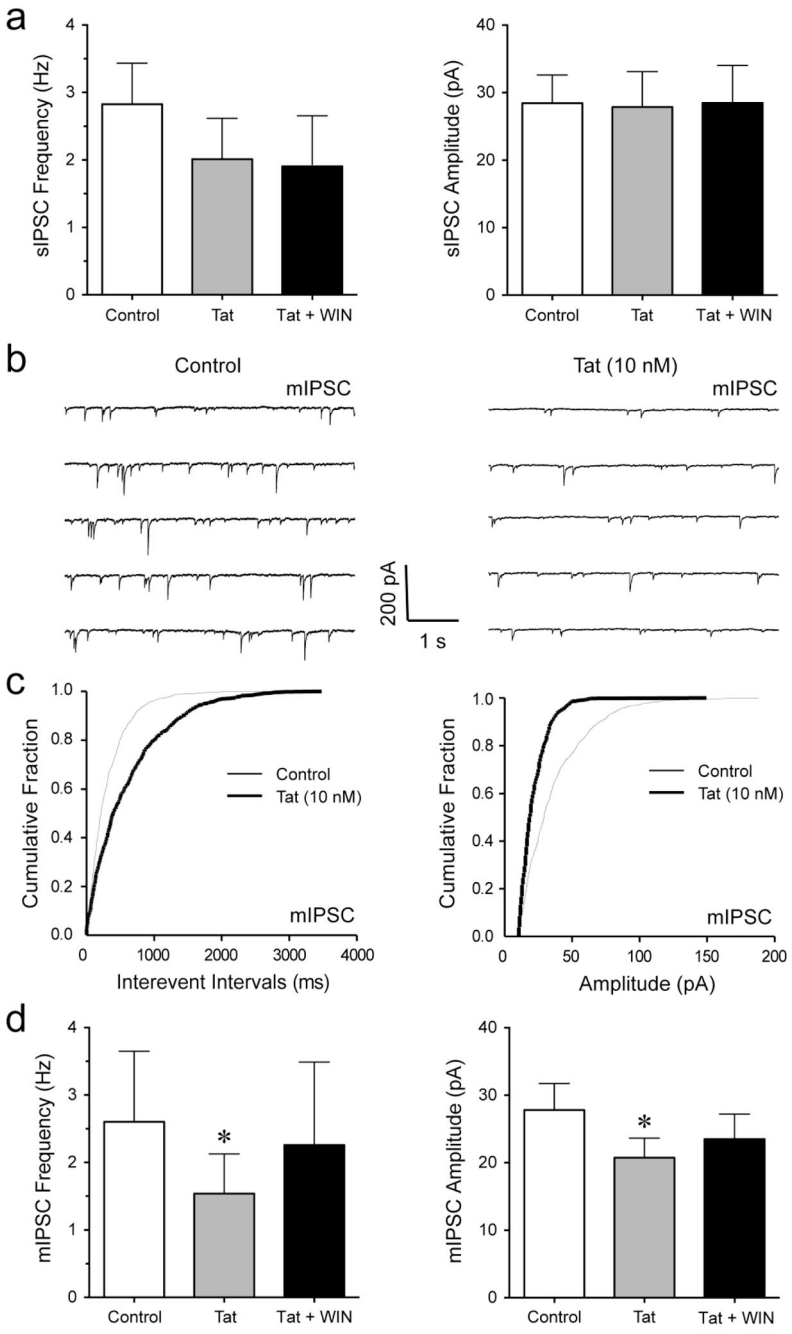

Figure 4. Tat significantly decreased the frequency and amplitude of mIPSCs in PFC pyramidal neurons, which was not affected after WIN55,212-2 treatment

(a) No significant differences were found in the mean frequency and amplitude of sIPSCs before and after the application of Tat (10 nM) or Tat + WIN55,212-2 (1 μM) ($n = 7$). (b) Representative traces show mIPSCs before Tat (10 nM) and after Tat (10 nM) application. (c) Cumulative frequency and amplitude distributions of mIPSCs based on data shown in Panel b. Both frequency and amplitude distributions were statistically different under these two experimental conditions (before vs. after treatment of Tat (10 nM); $p < 0.00001$ using KS-T; 958 events analyzed for before and 500 events for after Tat treatment). (d) Tat (10

nM) significantly decreased the mean frequency and amplitude of mIPSCs with WIN55,212-2 (1 μM) not further diminishing the Tat-induced decrease in mIPSCs ($n = 5$). Data are mean ± SEM. Significance was assessed by paired Student *t*-tests. *$p < 0.05$ vs. Control. WIN: WIN55,212-2.

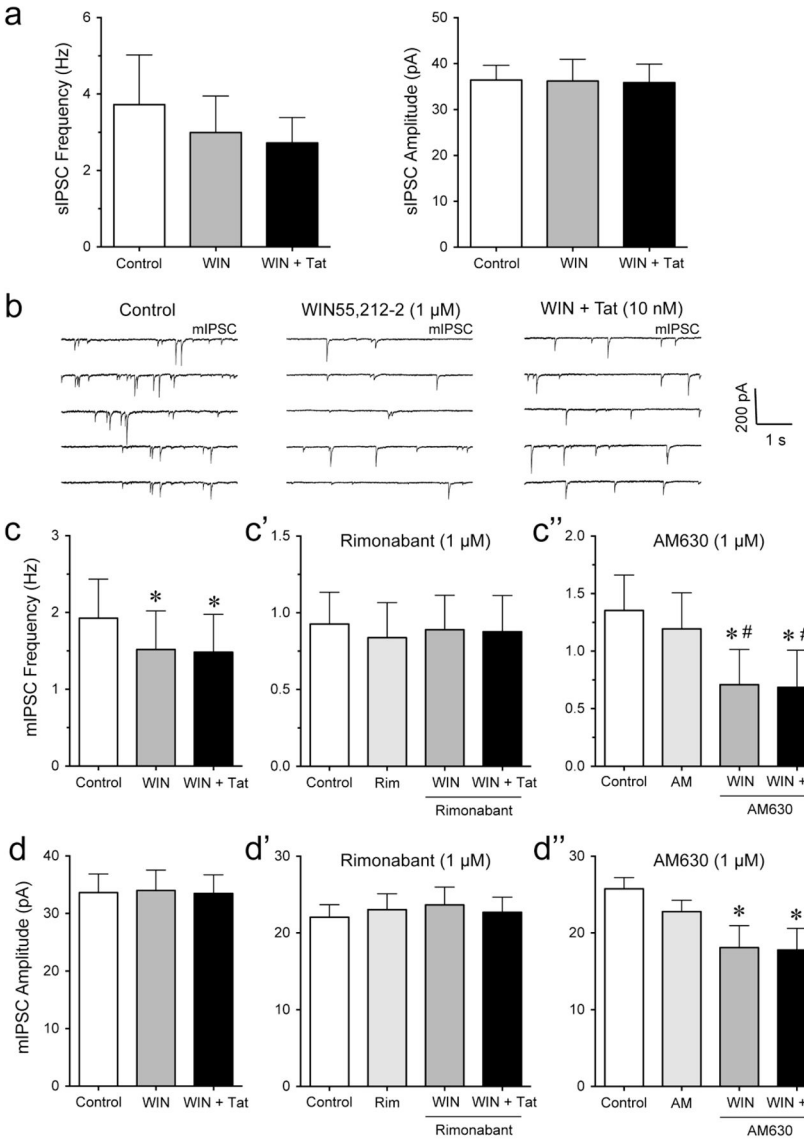

Figure 5. WIN55,212-2 significantly decreased the frequency but not amplitude of mIPSCs in PFC pyramidal neurons, which was blocked by rimonabant but not AM630

(a) WIN55,212-2 (1 μM) or WIN + Tat (10 nM) had no significant effect on the mean frequency and amplitude of sIPSCs ($n = 7$). (b) Representative traces show mIPSCs before WIN55,212-2 (1 μM), after WIN55,212-2, and after WIN + Tat (10 nM) application. (c, c′, c ″) Effects of WIN55,212-2 (1 μM) and Tat (10 nM) on the mean frequency of mIPSCs. WIN55,212-2 significantly decreased the mean frequency of mIPSCs with WIN + Tat not changing the WIN55,212-2-induced decrease in frequency of mIPSCs ($n = 7$, c). Pretreatment with rimonabant (1 μM) blocked the WIN55,212-2-induced decrease in the mean frequency of mIPSCs ($n = 9$, c′). Pretreatment with AM630 (1 μM) did not prevent the WIN55,212-2- and WIN + Tat-induced decreases in the mean frequency of mIPSCs ($n = 8$, c ″). (d, d′, d″) Effects of WIN55,212-2 (1 μM) and Tat (10 nM) on the mean amplitude of mIPSCs. WIN55,212-2 blocked the Tat-induced decrease in mean amplitude of mIPSCs ($n = 7$, d). No significant effects were noted when pretreating PFC slices with rimonabant (1 μM,

$n = 9$, d′). Pretreatment with AM630 (1 μM) significantly decreased the mean amplitude of mIPSCs for WIN55,212-2 and WIN + Tat compared to control ($n = 8$, d″). Data are mean ± SEM. Significance was assessed by paired Student *t*-tests. *$p < 0.05$ vs. Control, $^{\#}p < 0.05$ vs. AM (1 μM). WIN: WIN55,212-2; Rim: rimonabant; AM: AM630.

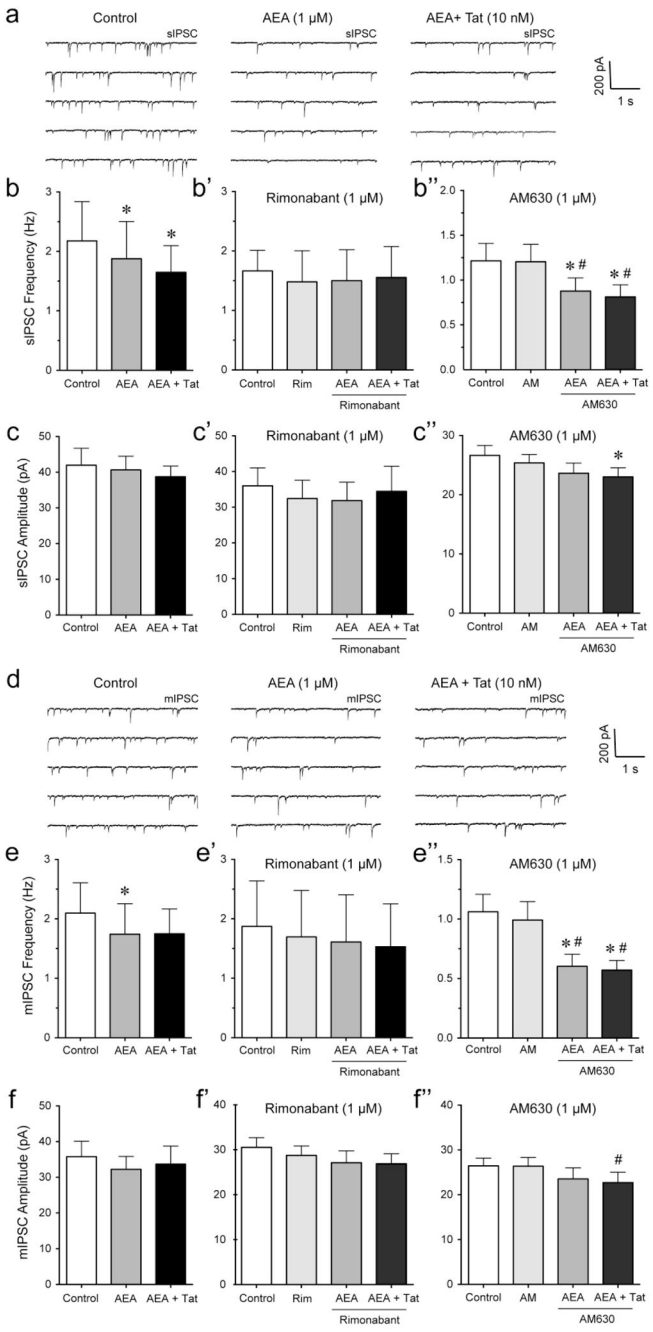

Figure 6. AEA significantly decreased the frequency but not amplitude of mIPSCs and sIPSCs in PFC pyramidal neurons, which was blocked by rimonabant but not AM630

(a) Representative traces show sIPSCs before AEA (1 μM), after AEA, and after AEA + Tat (10 nM) application. (b, b′, b″) Effects of AEA (1 μM) and Tat (10 nM) on the mean frequency of sIPSCs. AEA significantly decreased the mean frequency of sIPSCs with AEA + Tat not changing the AEA-induced decrease in frequency of sIPSCs ($n = 7$, b). Pretreatment of rimonabant (1 μM) blocked the AEA-induced decrease in the mean frequency of sIPSCs ($n = 5$, b′). Pretreatment of AM630 (1 μM) did not prevent the AEA− and AEA + Tat-induced decreases in the mean frequency of sIPSCs ($n = 10$, b″). (c, c′, c″)

Effects of AEA (1 μM) and Tat (10 nM) on the mean amplitude of sIPSCs. No effects were noted on the mean amplitude of sIPSCs in the absence ($n = 7$, c) or presence of rimonabant ($n = 5$, c′). Pretreatment of AM630 (1 μM) caused a significant decrease in the mean amplitude of sIPSCs by AEA + Tat compared to control ($n = 10$, c″). (d) Representative traces show mIPSCs before AEA (1 μM), after AEA, and after AEA + Tat (10 nM) application. (e, e′, e″) Effects of AEA (1 μM) and Tat (10 nM) on the mean frequency of mIPSCs. AEA significantly decreased the mean frequency of mIPSCs, whereas no further downregulation was noted for AEA + Tat ($n = 8$, e). Pretreatment of rimonabant (1 μM) blocked the AEA-induced decrease in the mean frequency of mIPSCs ($n = 5$, e′). Pretreatment of AM630 (1 μM) did not prevent the AEA− and AEA + Tat-induced decreases in the mean frequency of mIPSCs ($n = 11$, e″). (f, f′, f″) Effects of AEA (1 μM) and Tat (10 nM) on the mean amplitude of mIPSCs. No effects were noted on the mean amplitude of mIPSCs in the absence ($n = 8$, f) or presence of rimonabant ($n = 5$, f′). Pretreatment of AM630 (1 μM) caused a significant decrease in the mean amplitude of mIPSCs by AEA + Tat compared to AM630 alone ($n = 11$, f″). Data are mean ± SEM. Significance was assessed by paired Student *t*-tests. $^{*}p < 0.05$ vs. Control, $^{\#}p < 0.05$ vs. AM (1 μM), WIN: WIN55,212-2; Rim: rimonabant; AM: AM630.

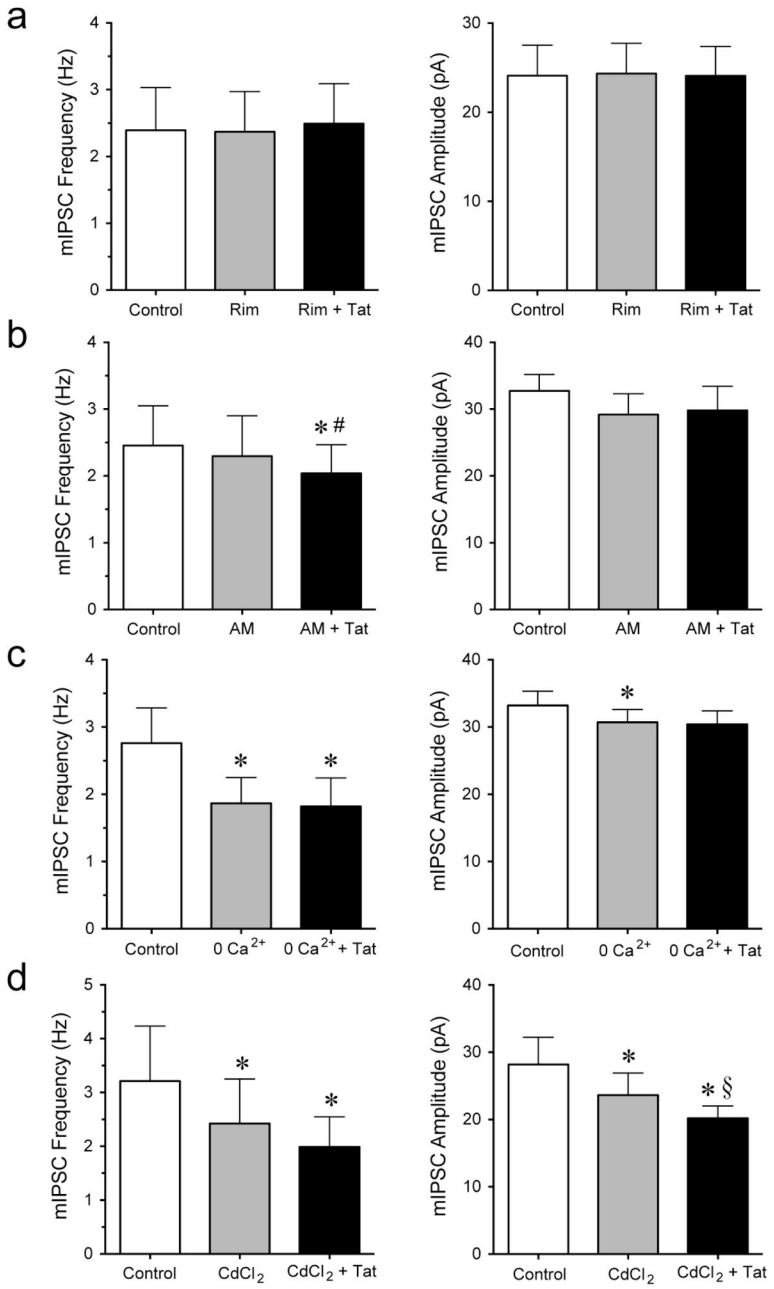

Figure 7. The significant effects of Tat on the frequency and amplitude of mIPSCs in PFC pyramidal neurons was blocked by CB_1R antagonist rimonabant and under conditions of zero extracellular Ca^{2+}

(a) Pretreatment of rimonabant (1 μM) blocked the Tat (10 nM)-induced decrease in the mean frequency and mean amplitude of mIPSCs ($n = 8$). (b) Pretreatment of AM630 (1 μM) did not block the Tat (10 nM)-induced decrease in the mean frequency of mIPSCs but prevented the Tat-induced decrease in the mean amplitude of mIPSCs ($n = 9$). (c) At zero extracellular calcium, Tat (10 nM) had no significant effect on mIPSC frequency and amplitude ($n = 7$). (d) In the presence of $CdCl_2$ (200 μM), Tat (10 nM) showed no significant effect on mIPSC frequency but decreased the mean amplitude of mIPSCs ($n = 6$). Data are

mean ± SEM. Significance was assessed by paired Student *t*-tests. *$p < 0.05$ vs. Control, $^{\#}p < 0.05$ vs. AM (1 μM), $^{\S}p < 0.05$ vs. $CdCl_2$ (200 μM). Rim: rimonabant; AM: AM630.